

## Supporting Information

### Conformational evolution following the sequential molecular dehydrogenation of PMDI on a Cu(111) surface

Lacheng Liu,<sup>a,b</sup> Alexander Timmer,<sup>a,b</sup> Elena Kolodzeiski,<sup>a,b</sup> Hong-Ying Gao,<sup>\*a,b,d</sup> Harry Mönig,<sup>a,b</sup> Henning Klaasen,<sup>c</sup> Xiangzhi Meng,<sup>a,b,e</sup> Jindong Ren,<sup>a,b,f</sup> Armido Studer,<sup>c</sup> Saeed Amirjalayer<sup>\*a,b</sup> and Harald Fuchs<sup>\*a,b</sup>

<sup>a</sup>Physikalisches Institut, Westfälische Wilhelms-Universität, Wilhelm-Klemm-Straße 10, 48149 Münster, Germany.

<sup>b</sup>Center for Nanotechnology (CeNTech), Heisenbergstraße 11, 48149 Münster, Germany. E-mails:

gaohongying@tju.edu.cn, samir\_01@uni-muenster.de, fuchsh@uni-muenster.de.

<sup>c</sup>Organisch-Chemisches Institut, Westfälische Wilhelms-Universität Münster, Corrensstraße 40, 48149 Münster, Germany.

<sup>d</sup>School of Chemical Engineering and Technology, Tianjin University, 300072 Tianjin, China.

<sup>e</sup>Institut für Experimentelle und Angewandte Physik, Christian-Albrechts-Universität zu Kiel, Leibnizstraße 19, 24118 Kiel, Germany.

<sup>f</sup>CAS key laboratory of Nanophotonic Materials and Devices, CAS Key Laboratory of Standardization and Measurement for Nanotechnology, National Center for Nanoscience and Technology, Beijing 100190, P.R. China

## **Table of Contents**

1. A DFT calculated model of the self-assembly structure of PMDI
2. Extended analysis of additional STM results
3. Extended analysis of XPS measurements
4. Computational Details
5. References

## 1. A DFT calculated model of the self-assembly structure of PMDI

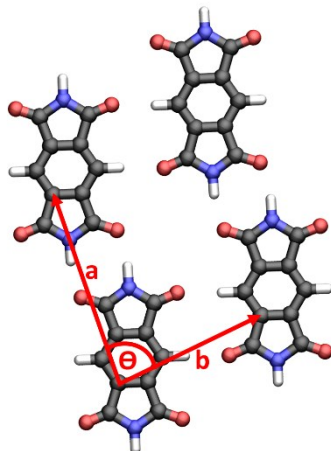


**Figure S1.** Ball-stick model of the DFT optimized geometry of four PMDI molecules in the gas-phase. (black: carbon atoms, white: hydrogen atoms, red: oxygen atoms, blue: nitrogen atoms). The theoretical model reveals the hydrogen bonding between the molecules leading to the experimentally observed self-assembly structure at the Cu surface.

## 2. Extended analysis of additional STM results

As mentioned in the main text, some molecules appear with a lower contrast compared with the molecules in the hydrogen bonded network were observed, when PMDI molecules as deposited on Cu(111) surface at room temperature (RT). It is more obvious in the overview STM image as shown in Figure S2a. There are more than 25% of the molecules with lower contrast (highlighted by purple circles in Figure S2b).

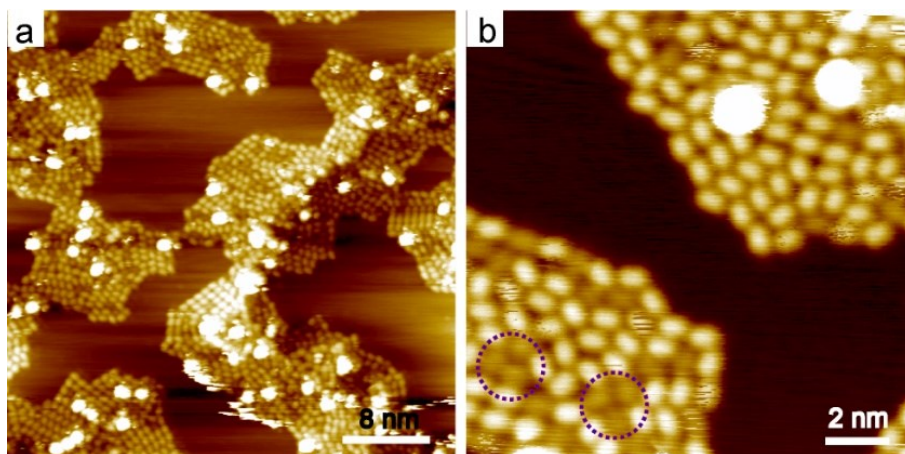


**Figure S2.** STM images of PMDI molecules as deposited on Cu(111) surface at RT. (a) Overview STM image (-2V, 10 pA,). (b) zoomed-in STM image (1.5V, 10 pA) The molecules with lower contrast than the intact ones are highlighted by purple circles.

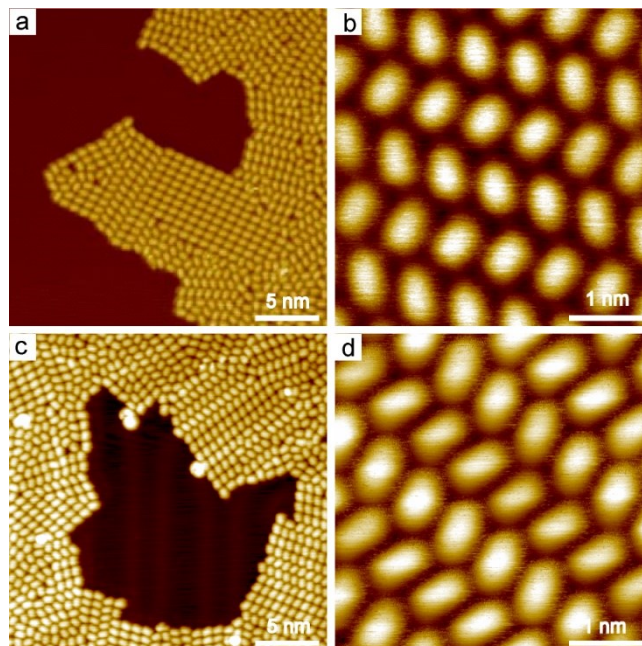


**Figure S3.** STM images of PMDI molecules on Ag(111) and Au(111) surfaces at room temperature. (a) Overview STM image of PMDI on Ag(111) (-0.5 V, 10 pA). (b) Zoomed-in STM of PMDI on Ag(111) (-0.6 V, 20 pA).. (c) Overview STM image of PMDI on Au(111) (1V, 50 pA). (d) Zoomed-in STM of PMDI on Au(111) (0.3V, 20 pA).

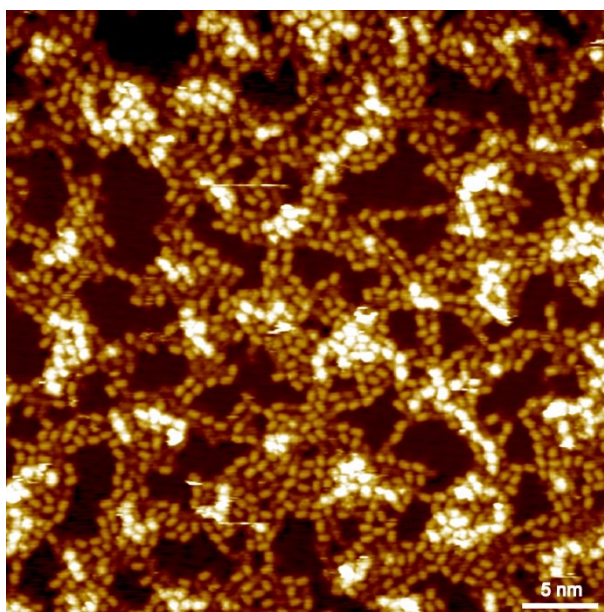


**Figure S4.** STM image of PMDI molecules on Cu(111) by cold deposition with high coverage (-0.5 V, 10 pA).

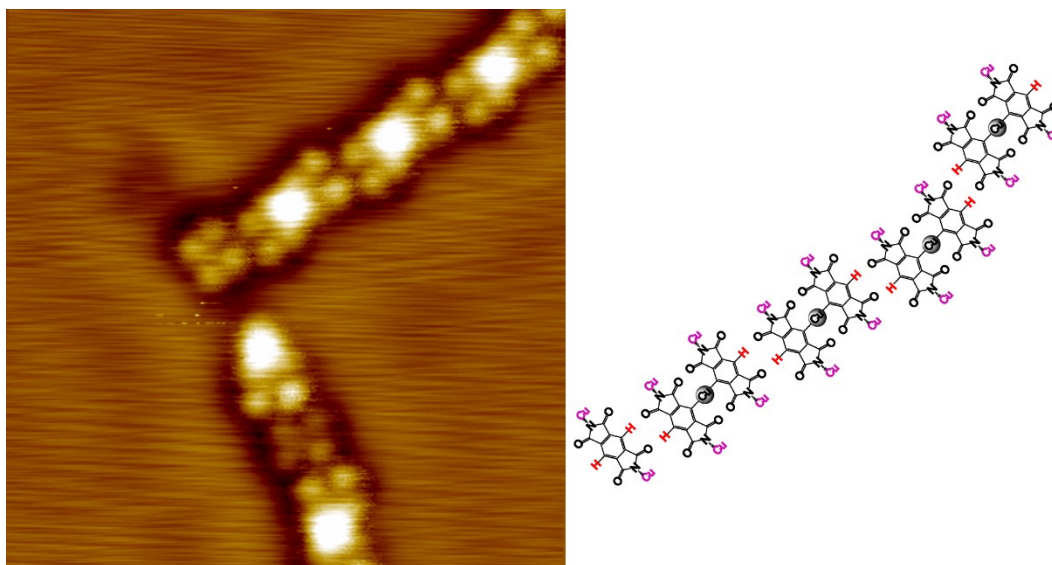


**Figure S5.** A sketch of linear structure formed by PMDI'-Cu dimers and PMDI' via C-H $\cdots$ O hydrogen bonding.

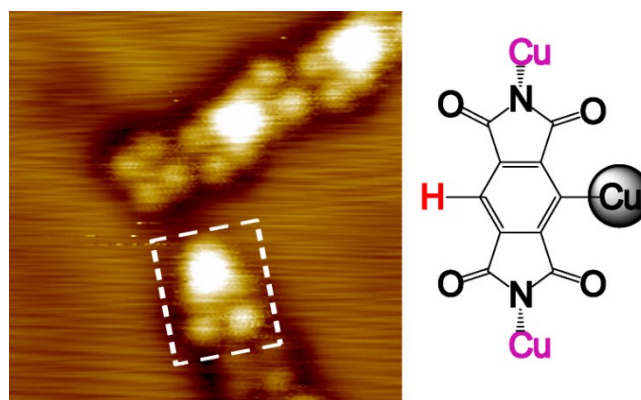


**Figure S6.** A schematic structure of PMDI'-Cu monomer on Cu(111) surface formed after annealing to 485K.

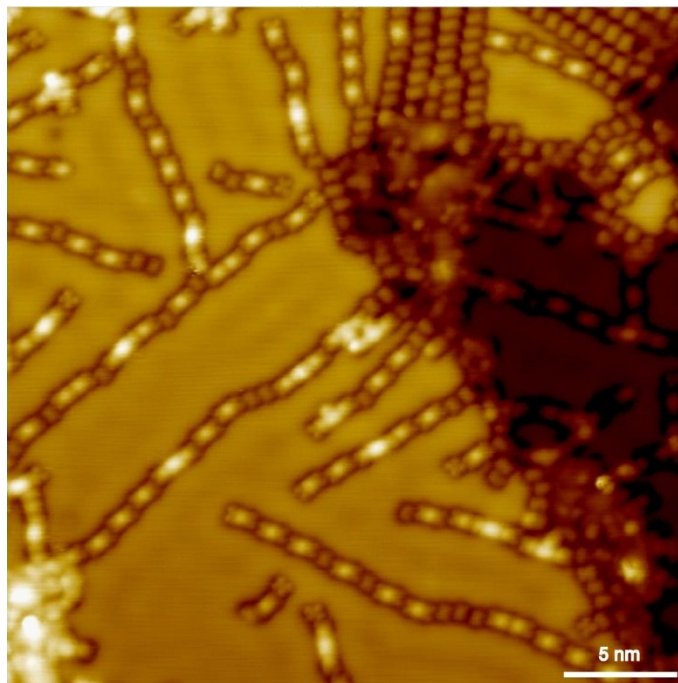


**Figure S7.** STM image of PMDI on Cu(111) surface after annealing to 505 K (-0.2 V, 20 pA).

### 3. Extended analysis of additional XPS measurements

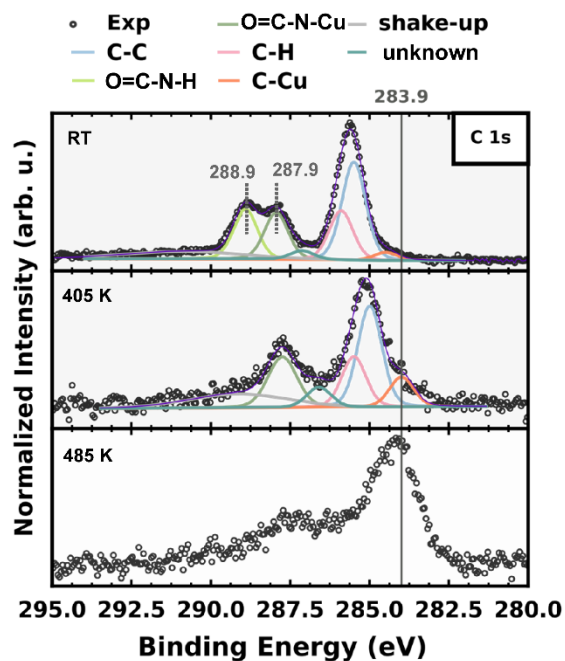


**Figure S8** X-ray photoelectron spectra and curve-fitting of the C 1s data of PMDI on Cu(111). From Top to bottom the data in each tile corresponds to the as deposited state at room temperature, first annealing step to 405 K and the final annealing step to 485 K, respectively. All sample states were checked by STM before the XPS measurements.

As shown in Figure S8, The C 1s spectrum of PDMI deposited at room temperature can be deconvoluted with six signals at binding energies of 285.5 eV (blue), 285.8 eV (pink), 287.1 eV (dark green), 287.9 eV (green), 288.9 eV (bright green) and 284.4 eV (orange) which can be attributed to the contributions of aromatic, peripheral carbon (C-H), an unspecific species (small dark green peak), carbon bound to nitrogen with hydrogen (bright green) and nitrogen with Cu at the surface (green) atoms and carbon bound to surface copper atoms (orange). A peak at the low BE side (orange) of the main carbon peak is commonly considered a strong indication for the formation of organometallic bonds. Upon further annealing to 405 K the peak corresponding to those carbon atoms bound to N-H is gone and the C-Cu component increases. The peak envelope after annealing to 485 K is increasingly complicated and conclusive peak fit analyses is not possible. The obvious broadening and shift towards lower BE of the C 1s peak is however conclusively explained by the formation of a significant amount of organometallic bonds (grey line).

#### 4. Computational Details

The DFT calculations are based on the Vienna Ab Initio Simulation Package (VASP)<sup>1,2</sup> with the optPBE-vdw functional and projected augmented wave (PAW) pseudo-potentials. The plane wave energies are limited by a cut-off energy of 400 eV. The standard deviation for the gaussian distribution approximating electronic states is 0.2 eV. As convergence criterion for the forces on the nuclei 0.02 eV/Å and for the electronic relaxation 10<sup>-7</sup> eV is set. The brillouin zone integration is performed on a 1x1x1 k-point grid. The model system consists of a unit cell, containing three 8x8 Cu-layers with a lattice constant of 3.65 Å and the investigated molecules on top of the surface. The periodic pictures of the model system in z-direction are separated by a 40 Å vacuum layer. The molecules adsorbed on the surface and the upper two layers were fully relaxed during the geometry optimizations. The tetramer configuration shown in Figure S1 is optimized using the B3LYP+D3 functional together with the def-SV(P) basis set both as implemented in the TURBOMOLE code<sup>3</sup>.

#### 5. Reference

1. G. Kresse, J. Furthmüller, *Phys. Rev. B* 1996, **54**, 11169-11186.
2. G. Kresse, J. Furthmüller, *Comput. Mater. Sci.* 1996, **6**, 15-50.
3. Turbomole 6.1: A development of University of Karlsruhe and Forschungszentrum Karlsruhe GmbH, Turbomole GmbH, 2009.